Compton Scattering of Gamma Rays

Jade Chongsathapornpong[1] and Kiran Mak[2]
[1] *MIT Department of Physics*
[2] *MIT Department of Materials Science*
(Dated: January 6, 2023)

A pair of scintillator detectors with coincidence gating measures the energies and flux of scattered ^{137}Cs gamma rays as a function of scattering angle. Gamma rays with reduced energies are observed, indicating an inelastic scattering process identified with Compton scattering. Qualitatively, observed angular dependence of scattered photon energies agrees with Compton scattering theory. However, the associated Compton wavelength of the electron is found to be $(2.071 \pm 0.074_{\text{stat}} \pm 0.112_{\text{sys}}) \times 10^{-12}$m, which disagrees with the accepted value at the 2.5-σ level. The observed angular dependence of scattering rates in these measurements is compared to Thomson and Klein-Nishina scattering predictions, with inconclusive results. We discuss means of ameliorating these measurements and potential corrections to their analysis, and present general considerations for similar experiments.

I. INTRODUCTION

Classical wisdom held light as a wave. However, Einstein's 1905 explanation of the photoelectric effect and accounts of the hydrogen spectrum presented in 1913 by Bohr began to elucidate light's discrete quantum nature. In the 1920s, Arthur Compton measured the spectra of scattered X-rays. He found that X-rays scattered at larger angles shifted systematically toward longer wavelengths, indicating a loss of energy. The wavelength shift was well-described by a quantum treatment of light as massless relativistic particles scattering from electrons while conserving energy and momentum [1].

This work follows in Compton's footsteps, using a gamma ray source irradiating a pair of scintillator targets. The energies corresponding to scattering events at chosen angles are recorded, while background radiation is mitigated via coincidence gating. We employ this setup to ascertain the angular dependence of gamma ray scattering energies to validate Compton's theory, specifically finding a linear relation between reciprocal scattered gamma ray energy and $(1 - \cos\theta)$, and extracting the Compton wavelength. Additionally, our setup provides a facile proxy to the gamma ray flux at a scintillator, allowing recovery of the scattering cross section of electrons by observing beam attenuation in samples of known composition. This latter study is presented in a companion paper by K. Mak [2].

II. THEORY

II.1. The Compton Shift

In relativistic mechanics, the energy-momentum relation links a particle's mass at rest m_0, its momentum p, and its total energy E given the speed of light c:

$$E^2 = p^2c^2 + (m_0c^2)^2 \tag{1}$$

In any scattering process, the total energy and momentum of a system are conserved between initial and final states. For a gamma ray scattering off an electron,

$$E_\gamma + E_e = E_{\gamma'} + E_{e'}, \quad \text{and} \quad \vec{p_\gamma} + \vec{p_e} = \vec{p_{\gamma'}} + \vec{p_{e'}} \tag{2}$$

where E_γ and $E_{\gamma'}$ are the initial and final energies of the gamma ray, and likewise E_e and $E_{e'}$ for the electron. The conservation of the total momentum $\vec{p}$ is analogous.

If we assume the electron begins approximately at rest and is accelerated to relativistic speeds after the scattering, the first equation becomes

$$E_\gamma + m_ec^2 = E_{\gamma'} + \sqrt{p_{e'}^2c^2 + (m_ec^2)^2} \tag{3}$$

with $p_{e'} = ||\vec{p_{e'}}||$. The second equation becomes

$$\vec{p_\gamma} - \vec{p_{\gamma'}} = \vec{p_{e'}} \tag{4}$$

This system of equations is in too many variables to yield clear relations. Compton's key insight was to treat the gamma ray as a massless particle, meaning $E_\gamma^2 = p_\gamma^2c^2$. This can be substituted into 3, eliminating E_γ and $E_{\gamma'}$. By then squaring both sides of 3 and 4 and subtracting according to [1], we arrive at

$$m_ec(p_\gamma - p_{\gamma'}) = p_\gamma p_{\gamma'} - \vec{p_\gamma} \cdot \vec{p_{\gamma'}} \tag{5}$$

Given $E = pc$, the momenta can be replaced by wavelength λ via the quantum description of light as photons, where $E = hc/\lambda$, with h being the Planck constant. Further manipulation of 5 yields the Compton formula for wavelength shift,

$$\lambda' - \lambda = \frac{h}{m_ec}(1 - \cos\theta) \tag{6}$$

The quantity h/m_ec is known as the Compton wavelength λ_c of the electron.

As a note, the intensity distribution of scattered photons is predicted by the Klein-Nishina formula, derived in the framework of relativistic quantum mechanics [3]. This differential scattering cross section is

$$\frac{d\sigma}{d\Omega} \propto \left(\frac{\lambda}{\lambda'}\right)^2 \left[\left(\frac{\lambda}{\lambda'} + \frac{\lambda'}{\lambda}\right) - \sin^2\theta\right] \tag{7}$$

where θ is the angle by which a photon is scattered from its original direction.

II.2. Thomson Scattering

When $\lambda \gg \lambda_c$, the oscillating electric field of light as an electromagnetic wave accelerates charged electrons, which in turn radiate. Consider waves incident on an electron, as in Fig. 1, and an observer in the figure plane. Unpolarized light is a superposition of two orthogonal polarization components, one in the figure plane as shown, and the other into/out of the page. The electron motion due to the electric field can be likewise decomposed.

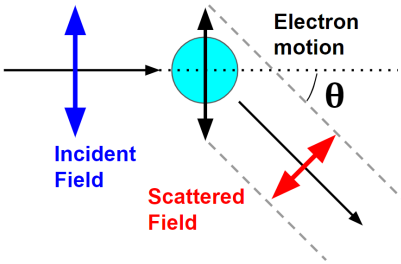

FIG. 1. Illustration of Thomson scattering, adapted from [].

To the observer, the amplitude of motion in the plane, and the corresponding radiated field amplitude, is by inspection proportional to $\cos\theta$. Meanwhile, the motion due to the component *into* the plane is not affected in this way. Thus, the total amplitude observed is proportional to $\sqrt{1+\cos^2\theta}$, whose square is the intensity. This leads to the Thomson differential cross section,

$$\frac{d\sigma_T}{d\Omega} \propto \left(1+\cos^2\theta\right) \tag{8}$$

which disagrees for high energies with the Klein-Nishina prediction, and prescribes no wavelength shift.

III. APPARATUS

The experimental apparatus revolves around a circular table. Two 2×2-in cylindrical sodium iodide (NaI) scintillators coupled to photomultiplier tubes serve as gamma ray detectors which resolve energies. One detector ("recoil") is at the table center, and the other ("scatter") is at the table edge, 25cm away. To the side, a sample of ^{137}Cs is enclosed in lead with a roughly 1cm aperture. The output beam of 662 keV photons is directed at the recoil detector, where some gamma rays undergo Compton scattering, dissipating energy. Some scatter into the scatter detector and are absorbed. These events reveal the energies involved in Compton scattering.

An array of supporting electronics, outlined in 2, energizes the detectors' photomultiplier tubes and processes their output. Pulses from each detector are amplified, before being sent to a multichannel analyzer (MCA) which counts the pulses in one of 2048 bins according to their size. However, as the experiment is unshielded, many

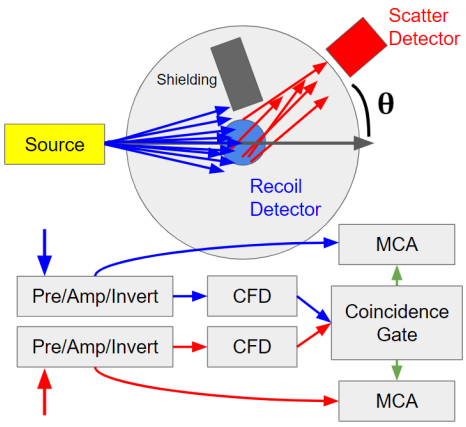

FIG. 2. Block diagram of setup, adapted from [1].

observations at each detector do not correspond to the events of interest which can be distinguished by virtue of occurring nearly simultaneously in both detectors. To this end, inverted copies of the amplified pulses are sent to constant fraction discriminators, which in turn produce precisely timed output pulses marking each sufficiently large pulse. These timing pulses are fed to a coincidence detector and gate generator which, on receiving temporally coincident pulses, produce a gate pulse informing the MCAs to record the corresponding events.

IV. MEASUREMENTS

For each experimental run, calibrations of MCA binning were performed. Coincidence gating was disabled, and a ^{133}Ba source was deployed. The detector voltages and amplifier gains were adjusted until the 356 keV peak was at half scale. Events were recorded until the histogram appeared smooth. Afterwards, discriminator thresholds and gate delays of the coincidence mechanism were validated using a ^{22}Na source, which produces simultaneous 511 keV photons traveling in opposite directions. When coincidence gating was enabled with discriminator thresholds sufficiently high to reject noise and gate delays capturing coincident peaks, negligible count rates (< 1/s) were observed except when the ^{22}Na source was placed on a straight line between detectors, as expected. The MCA histogram peaks of ^{133}Ba and ^{22}Na were matched to known spectra, and fit to a line through the origin as shown in Fig. 3, with uncertainties on the resulting keV/bin calibration estimated assuming peaks were Gaussian profiles, then varying the calibration constant until $\Delta\chi^2 = 1$. Typical statistical uncertainty thus calculated was 1.2%. Agreement with known spectra was typically within 2%. Systematic uncertainty was estimated by comparing the linear fit with calibration to only the highest-energy peak. This ranged from -0.4% to -3.5%, with an average of -2.1%, perhaps due to nonlinear detector response. This overall calibration uncertainty of

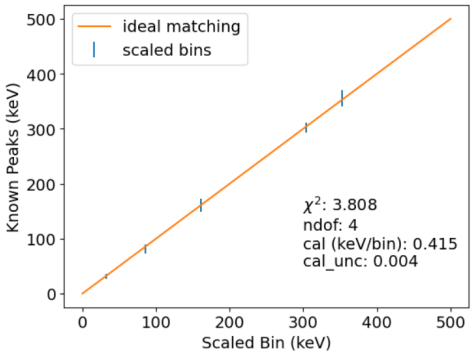

FIG. 3. Example calibration fit to ^{133}Ba. Agreement between expected peak energies and observations generally within 2%.

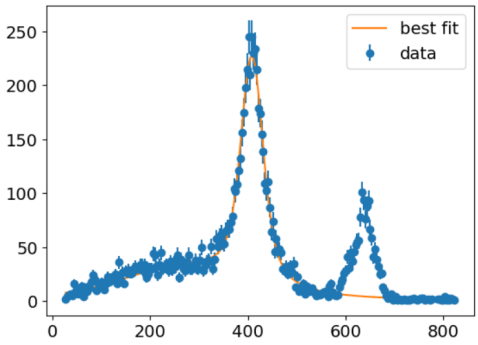

FIG. 4. Example of recoil energy peak fit to a sum of two Voigt profiles, for 120°. At 630 keV, another peak correspondds to accidentally coincident incoming photons.

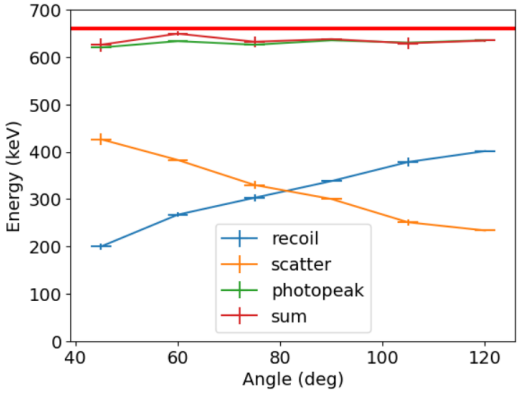

FIG. 5. Fitted peak energies of Compton scatter and recoil, their sums, and incoming photons, at different angles. The fitted incoming photon and Compton sum energies agree, but are approximately 5% lower than the expected energy.

2.4% affects final energies systematically.

After calibration, coincidence gating was enabled. The ^{137}Cs source was placed approximately 35cm away from the recoil detector. The long (beam direction) axis of the enclosure was visually aligned to the recoil detector and the 0° marking on the table using a straight edge, and it was assumed the beam axis was aligned with this axis. The approximate precision of this alignment was 2°, due largely to the awkward shape of the source and bench geometry making appropriate viewing angles difficult to access. Then, the scatter detector, itself approximately 25cm from the table center, was rotated to a given angle. Our apparatus had a somewhat tilted mount for the scatter detector, which made it difficult to determine the scintillator's center in the plane of the beam. Here, we also estimate the uncertainty on the resulting angle at 2°. With alignments completed, the source was opened, and counts were collected over approximately 30 minutes per angle, from 45 to 120 degrees off-axis.

V. DATA AND ANALYSIS

V.1. Energy Conservation

We expect recoil and scatter energies to sum to the initial photon energy. The events were re-binned into 128 bins, then scaled by energy calibrations. Uncertainties were estimated assuming Poisson statistics. The re-binned histograms were fit to the sum of two Voigt profiles. Though this choice is arbitrary, the fits captured the peak shapes, as demonstrated in Fig. 4. The energies extracted from the fits for recoil and scatter detectors, their sums, and the observed incoming photon energies chiefly from absorption events in the recoil detector which happened to coincide with other detections in the scatter detector, are plotted as a function of angle in Fig. 5.

Remarkably, despite our calibration from 30 to 511 keV, the sums and the incoming photon energies agree near 630 keV, below the 662 keV of ^{137}Cs gamma rays. This agreement even at different angles makes nonlinear detector response a poor explanation for the apparent energy loss. That said, the 5% difference is not so far from the 2% errors at individual spectral lines in calibration. The loss might also be an artifact of biases in event selection during coincidence-gated measurements. Including ^{137}Cs as a regular calibration source would detect this.

V.2. Angular Energy Dependence

Rewriting the Compton formula with $E = hc/\lambda$ indicates a linear relationship between reciprocal scattered photon energy and $(1 - \cos\theta)$:

$$\frac{1}{E_{\gamma'}} + \frac{1}{E_\gamma} = \frac{1}{m_e c^2}(1 - \cos\theta) \tag{9}$$

This, with corresponding data, are plotted in Fig. 6. Qualitatively, our data captures the prediction. For a quantitative result, a line was fit. Vertical pointwise uncertainties stem from energy fit uncertainties, and a re-binning uncertainty estimated by repeating the energy peak fit with 256 bins instead of 128, and seeing

the energy difference. Horizontal uncertainties due to scatter detector position were converted into vertical uncertainties by the slope of an initial linear least-squares fit, and added in quadrature. Then, a weighted linear least-squares fit was performed. The uncertainty on the extracted fit parameters was taken as statistical. Finally, systematic uncertainty from calibration was estimated by repeating this process assuming a calibration constant raised or lowered by its uncertainty, then taking the difference, and likewise for systematic uncertainty from source alignment. The slope was then scaled to afford the electron Compton wavelength:

$$\lambda_c = (2.071 \pm 0.074_{\text{stat}} \pm 0.112_{\text{sys}}) \times 10^{-12}\,\text{m}$$

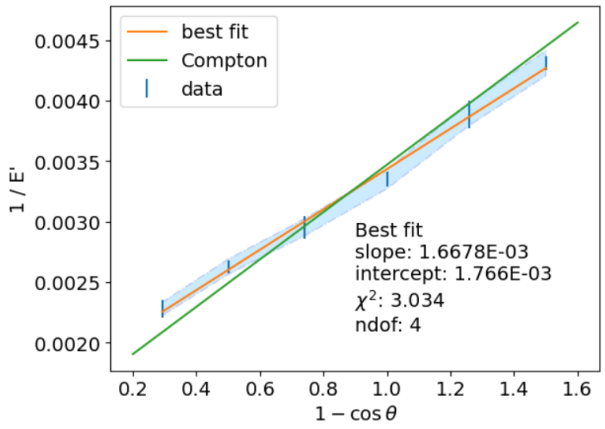

FIG. 6. Plot of $1/E_{\gamma'}$ vs. $(1-\cos\theta)$; prediction in green, fit in orange. Systematic uncertainty from calibration in light blue error bands. Vertical uncertainties: peak fitting and rebinning. Horizontal uncertainty: scatter detector positioning. Not pictured: systematic uncertainty from source alignment.

V.3. Differential Cross Sections

The Klein-Nishina formula predicts a strong bias missing in Thomson's model toward small-angle scattering of gamma rays. To attempt to verify this, counts within the full-width half maxima of Compton energy peaks in the recoil and scatter detectors were divided by integration times, to estimate count rates as a function of angle. Although this was not a robust approach, it was immediately discovered that data in these regions were polluted with background or accidental coincidences. If our coincidence gating were perfect, a near-one-to-one correspondence would exist between recoil and scatter detections in the Compton peaks. Instead, the calculated rates for a given angle varied by a factor ranging from 1.5 to 6 between the recoil and scatter detectors. This is strange, considering that we found our coincidence gating effective at suppressing ambient background. It is likely the large flux from the source at the recoil detector enabled background events to leak in via the scatter detector. Lacking a reasonable model for the background which results from this, we abandoned this analysis.

VI. CONCLUSIONS

We have shown the energies of scattered gamma rays are reduced in a manner reasonably consistent with Compton's treatment of the photon as a massless relativistic particle colliding with electrons. Our result for the electron Compton wavelength of $\lambda_c = 2071 \pm 135$nm, which is 2.6σ from the accepted value of 2426.31nm. Certainly, the Thomson description of scattering is inadequate, as it demands $\lambda_c = 0$, but regardless our discrepancy invites further investigation. The background present in our spectra discovered by inspecting rates also suggests apparatus improvements may be important.

Short of shielding the entire setup, employing a more intense and collimated source, more carefully tuning the coincidence gate, and shielding the scatter detector from all directions except the path to the recoil detector, should greatly improve signal-to-noise. Moreover, increasing the distances involved would, trading off signal-to-noise, improve angular resolution—currently, the fairly large detectors acquire Compton events over a range perhaps up to 10°. If the Klein-Nishina formula is correct, over this range, steep intensity gradients exist, with varying curvature. This would individually bias the "real" angle being measured at each detector angle, contributing an error we have not accounted for. Additionally, higher order scattering may still trigger coincidences, with unclear overall effects. A Monte Carlo simulation of these phenomena and the expected spectra that would result from them is in progress, and will hopefully yield deeper insights into our data.

ACKNOWLEDGEMENTS

I would like to thank Kiran Mak for her assistance, especially in running experiments and providing food while I was sick for a week. J-Lab staff, besides helping with the setup, also contributed feedback for which I am grateful.

[1] D. o. P. MIT, "Compton scattering manual," (2013).
[2] K. Mak, 8.13 Procedia (2022).
[3] Y. Yazaki, Proceedings of the Japan Academy, Series B **93**, 399 (2017).